1

Macroscale Hydrological Modeling and Global Water Balance

Taikan Oki and Hyungjun Kim

ABSTRACT

An overview of the global hydrological cycle, and recent achievements in macroscale modeling are given. Major components of fluxes and storages in the global hydrological cycle are described and quantitatively illustrated based on an off-line simulation framework. Methodologies for estimating fluxes and storage changes are presented from the simple water balance concept to the state-of-the-art numerical models that are capable of incorporating anthropogenic impacts. Efforts made by international research communities on global-scale hydrologic modeling are introduced. Current situations of modeling, research opportunities, and gaps in global hydrology are also identified.

1.1. INTRODUCTION

"Blue Planet" is a frequently used term to describe the Earth, as approximately 70% of its surface is covered by water. Although the water mass constitutes only 0.02% of the total mass of the planet (5.974×10^{24} kg), it is a critical matter for all organisms including humans in their survival [*Oki et al.*, 2004]. Also, its availability has largely affected civilizations in both culture and economy in human history. Therefore, to ensure adequate fresh water supply is essential for human well-being.

The Earth's surface is dominated by various forms of water. The total volume of water on the Earth is estimated to be approximately 1.4×10^{18} m^3, which corresponds to a mass of 1.4×10^{21} kg. The global hydrologic cycle always includes the oceanic circulation. The proportion of water in the ocean is large (96.5%). Oceanic circulations carry large amounts of energy and water. The surface ocean currents are driven by surface wind stresses, and the atmosphere itself is sensitive to the sea surface temperature. Temperature and salinity together determine the density of ocean water, and both factors contribute to the overturning and the ocean general circulation. Some terrestrial areas are covered by freshwater (lakes and rivers), solid water (ice and snow), and vegetations (which imply the existence of water). Even though the water content of the atmosphere is relatively small (approximately 0.3% by mass and 0.5% by volume), 0.68 (±0.03)% of the area above the Earth is always covered by clouds when considering clouds with optical depth > 0.1 [*Stubenrauch et al.*, 2013].

Water on the Earth is stored in various reservoirs, and water flows from one to another. Water flow per unit time is also called water flux. To understand the global water cycle, the quantification of fluxes and storages with the associated processes is necessary. Figure 1.1 schematically illustrates various water storages and fluxes in the global hydrologic system [revised from *Oki and Kanae*, 2006].

The objective of this chapter is to give a brief overview of research approaches for global water-balance estimation. To provide basic background of the water cycle, in Section 1.2, major components of terrestrial hydrologic processes are briefly explained with quantitative estimations using a global off-line simulation. From Section 1.3 to Section 1.5, the major methodologies for water-balance estimations are described. An early estimation that used reanalysis data set and a simple water-balance equation is introduced, and the development of the model-based macroscale land simulation framework and recent achievements to consider the human impact are covered.

Institute of Industrial Science, The University of Tokyo, Tokyo, Japan

Terrestrial Water Cycle and Climate Change: Natural and Human-Induced Impacts, Geophysical Monograph 221, First Edition.
Edited by Qiuhong Tang and Taikan Oki.

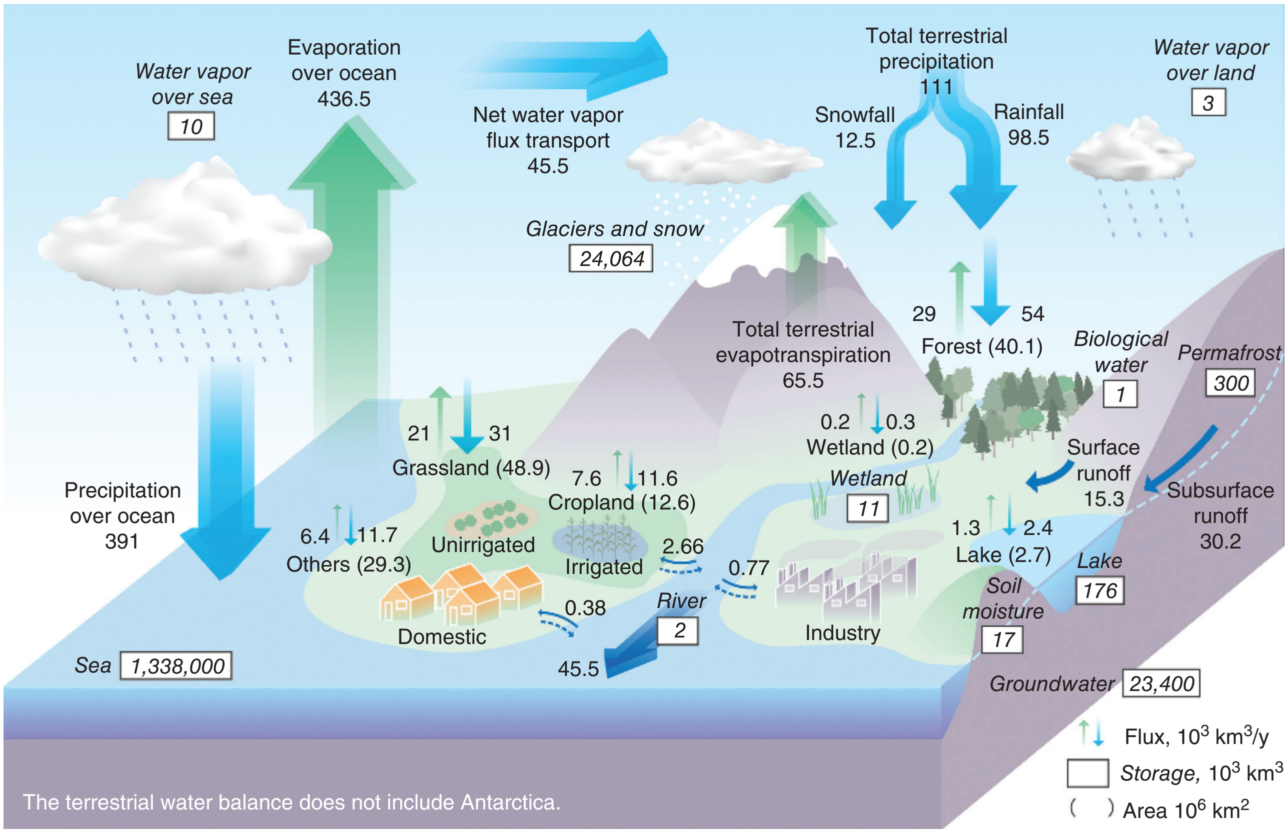

Figure 1.1 Global hydrological fluxes (1000 km^3 yr^{-1}) and storages (1000 km^3) with natural and anthropogenic cycles are synthesized from various sources. Vertical arrows show annual precipitation and evapotranspiration over ocean and land with major landscapes (1000 km^3 yr^{-1}). Parentheses indicate the area (million km^2) [from *Oki and Kanae*, 2006].

Section 1.6 introduces how the science communities have organized international collaborative frameworks. As the last part, prospects for macroscale hydrologic model development in the near future are given in Section 1.7.

1.2. COMPONENTS OF TERRESTRIAL HYDROLOGICAL CYCLES

Precipitation is the water flux from the atmosphere to the land or the ocean surface. It drives the hydrological cycle over the land surface and also changes the ocean surface physical properties (i.e., salinity and temperature), which affect its thermohaline circulation. It is intercepted by vegetation canopy, and the amount exceeding the interception storage reaches the land surface as throughfall. Compared to the other major hydrological fluxes, precipitation behaves in a more variable, intermittent, and concentrated way in time and space. Despite dense gauge station networks, such a highly inhomogeneous spatiotemporal variability makes the observation of precipitation and the aggregation of the process complicated and challenging. In a hybrid product, such as Global Precipitation Climatology Project (GPCP) [*Huffman et al.*, 1997], satellite-based estimates are merged with in situ observational data to fill the observational gaps. Global distribution of precipitation is presented in Figure 1.2a.

Snow has special characteristics compared to rain which refers to the liquid phase of precipitation. When snow accumulates, the surface temperature keeps 0 °C or below until the completion of snow melt. The albedo of new snow can be as high as cloud albedo, and it varies between 0.6 and 0.9 in the aging process (covered with dust). Consequently, the existence of snow significantly changes the surface budget of energy and water. A snow surface typically reduces the aerodynamic roughness, so that it may also have a dynamic effect on the atmospheric circulation and associated local and remote hydrologic cycles.

Evapotranspiration, consisting of evaporation and transpiration, is the flow of water and latent heat energy returning from the surface to the atmosphere. The amount of evaporation is determined by both atmospheric and hydrological conditions. Wetness at the surface influences the partition between latent and sensible heat significantly.

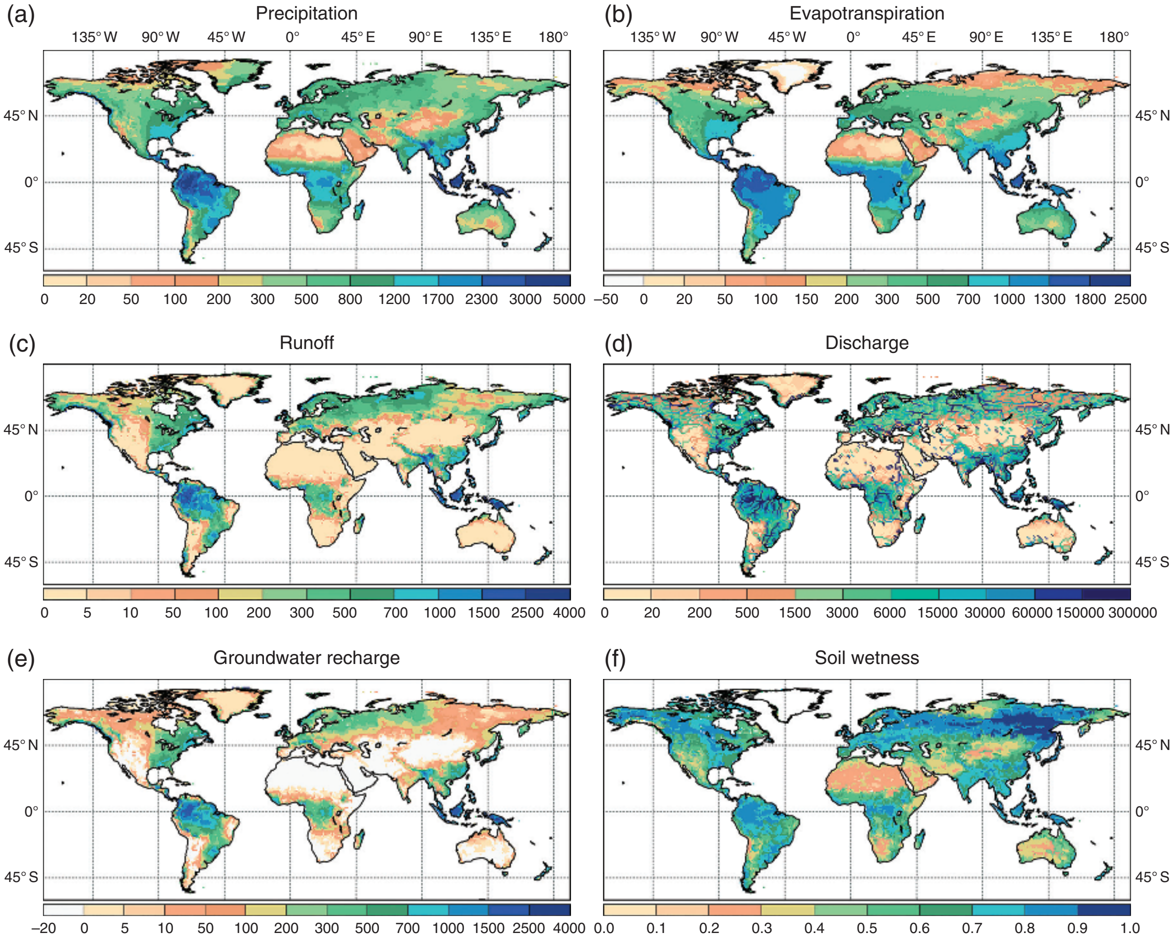

Figure 1.2 Global distribution of long-term (1979–2013) annual mean of (a) precipitation (mm yr^{-1}) from the GPCC [*Schneider et al.*, 2014], (b) evapotranspiration (mm yr^{-1}), (c) runoff (mm yr^{-1}), (d) river discharge (m^3 yr^{-1}), (e) groundwater recharge (mm yr^{-1}), and (f) soil wetness (-) from off-line hydrological simulations by Ensemble Land Surface Estimator (ELSE) [*Kim and Oki*, 2014].

The ratio of actual evaporation to potential evaporation is reduced due to drying stress near the surface. The stress is sometimes formulated as a resistance under which evaporation is classified as hydrology-driven (soil-controlled). If the land surface is wet enough compared to available energy for evaporation, the condition is classified as radiation driven (atmosphere controlled).

Transpiration is the release of water vapor from the stomata of leaves. It is distinguished from evaporation from soil surfaces in two aspects. One is that the resistance of stomata does not relate only to the soil dryness but also to the physiological conditions of vegetation through the opening and closing of stomata. The other is that roots can transfer water from deeper soil layers in contrast to evaporation over bare soil. Vegetation also modifies the balance of surface energy and water by altering surface albedo and by intercepting and evaporating a part of precipitation. The global distribution of total evapotranspiration is shown in Figure 1.2b.

Runoff (Fig. 1.2c) carries water back to the ocean from the land. Without rivers, global hydrologic cycles on the Earth are not closed. Runoff into the ocean also plays a role in the freshwater balance and the salinity of the ocean. Rivers carry not only water but also sediments, chemicals, and various nutrient materials from continents to seas. Runoff at the hillslope scale is a nonlinear and complex process. Surface runoff can be generated when the intensity of rainfall or snowmelt exceeds the infiltration capacity of the soil (Hortonian runoff), or when rain falls on the saturated land surface (Dunne runoff).

Saturation at the land surface mostly occurs along the hill slopes according to the topographic concentration mechanism. Infiltrated water in the upper part of the hill slope flows down the slope and discharges at the bottom of the hill. Because of the high heterogeneity of topography, soil properties (such as hydraulic conductivity and porosity), and precipitation, basic equations such as Richard's equation, which can be valid fairly well at a point scale or hillslope scale, cannot be directly applied in the macroscale using the mean quantities because of the nonlinearity involved. The river discharge accumulates total runoff generated in upstream watershed. The global distributions of runoff and river discharge are illustrated in Figure 1.2c and d.

Groundwater is the subsurface water in the saturated zone. It contributes to the runoff in the low-flow regime between storm events, that is, during a dry spell. Deep groundwater may also reflect the long-term climatological condition. The groundwater quantity in Figure 1.1 considers both gravitational and capillary water, but groundwater in Antarctica (roughly estimated as $2 \times 10^6\,\mathrm{km}^3$) is excluded. Gravitational water is the water in the unsaturated zone (vadose zone), which moves downward by gravity. Capillary water is the water that moves upward due to capillary diffusion. Implementing macroscale groundwater dynamics, *Koirala* [2010] estimated groundwater recharge flux as $31{,}789\,\mathrm{km}^3\,\mathrm{yr}^{-1}$, which is close to the flux of subsurface runoff in Figure 1.1 ($30{,}200\,\mathrm{km}^3\,\mathrm{yr}^{-1}$). The global distribution of model-simulated groundwater recharge is illustrated in Figure 1.2e.

The global distribution of soil wetness is shown in Figure 1.2f. Soil moisture is the water being held above the groundwater table. It influences the energy balance at the land surface by affecting evapotranspiration (which consists of soil evaporation, plant transpiration, and interception loss) and changing surface albedo. Soil moisture also alters the fraction of precipitation partitioned into direct runoff and infiltration. When the temperature of the soil column keeps at or below 0 °C for more than two consecutive years, the condition is called permafrost. During the summer season, the upper part of the soil column thaws and the melting water infiltrates downward, but the permafrost layer is still impermeable like a bedrock. Figure 1.3 indicates the global estimation of evapotranspiration and runoff. Approximately one third of precipitation turns to runoff and one third of the runoff is estimated to be surface runoff. The shares of transpiration, canopy infiltration, and bare soil evaporation are close on global average.

Major reserves other than the ocean are solid waters on the continent, including glaciers and permanent snow cover. Glaciers are ice accumulations originated from the atmosphere, and they move slowly on land over a long time period. Glaciers form U-shaped valleys over land and leave moraine deposits when they retreat. If a glacier "flows" into an ocean, it often turns into an iceberg. Glaciers evolve in a relatively longer timescale in comparison to climatic change. They can also induce isostatic responses of continental-scale upheavals or subsidence in even longer timescales. Even though it was believed that the thermal expansion of oceanic water dominated the anticipated sea level rise due to global warming, glaciers over land are also a major concern as the cause of sea level rise associated with global warming in the coming decades.

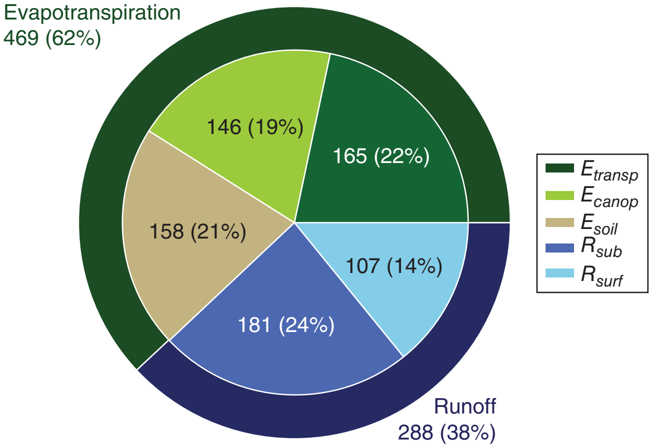

Figure 1.3 Global water balance and partitioning between the components of evapotranspiration (E_{transp}: transpiration, E_{canop}: interception-loss, and E_{soil}: evaporation from bare soil) and runoff (R_{surf}: surface runoff, R_{sub}: base flow) based on the estimation by *Kim and Oki* [2014].

1.3. GLOBAL WATER BALANCE IN EARLY ERA

The 1980s was the dawn of four-dimensional data assimilation (4DDA) of the global atmosphere. *Oki et al.* [1995] were one of the first to demonstrate the potential capability of 4DDA data to estimate terrestrial water balances using global precipitation observations and large basin river discharges based on the atmospheric water balance (AWB) method. Water balance over land and combined water balance are schematically illustrated in Figure 1.4.

The water balance over land is described as equation (1.1) where P, E, R, and S are precipitation, evapotranspiration, runoff, and terrestrial water storage, respectively, within an arbitrary boundary as illustrated in Figure 1.4a:

$$\frac{dS}{dt} = P - E - R \tag{1.1}$$

Atmospheric water vapor flux convergence contains water balance information in addition to the traditional hydrological elements such as precipitation, evapotranspiration, and discharge. The basic concepts as well as the application of atmospheric data to estimate terrestrial water balance were first presented by *Starr and Peixöto* [1958]. The atmospheric water balance for a column of atmosphere from the bottom at land surface to the top of the atmosphere is described by the equation,

$$\frac{dW}{dt} = Q + \left(E - P\right) \tag{1.2}$$

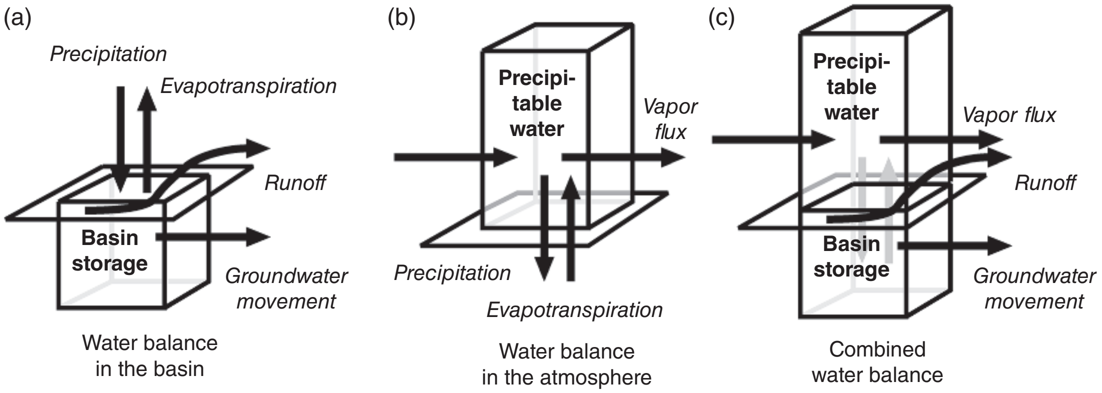

Figure 1.4 Schematic diagram for (a) terrestrial water balance, (b) atmospheric water balance, and (c) combined atmosphere–land surface water balance corresponding to equations (1.1), (1.2), and (1.3), respectively [*Oki et al.*, 1995].

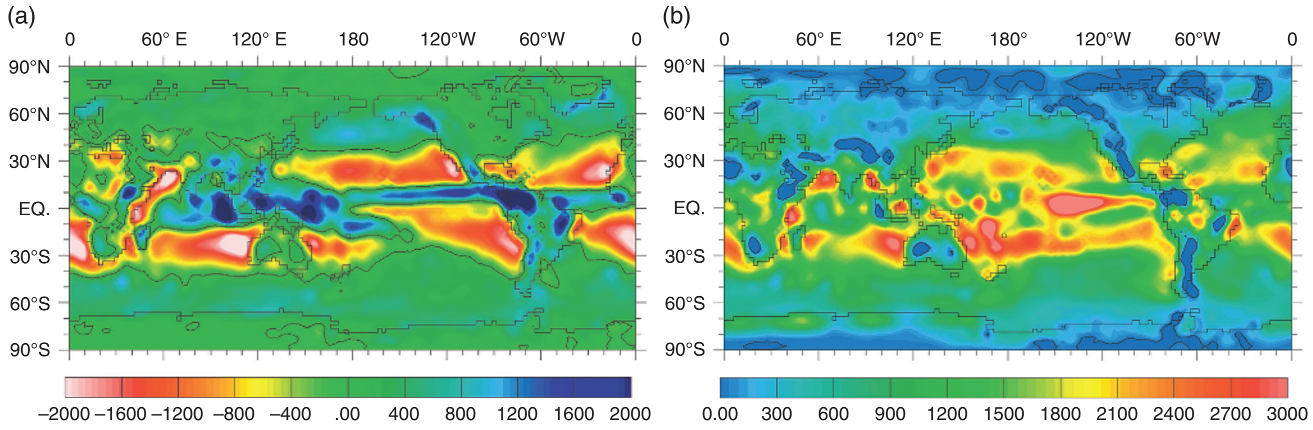

Figure 1.5 Atmospheric water balance approach using (a) annual vapor-flux convergence (mm yr^{-1}) from European Centre for Medium-Range Weather Forecast (ECMWF) global analysis [*Hoskins*, 1989] based on *Oki et al.* [1995] to estimate (b) annual mean evapotranspiration (mm yr^{-1}) for 1989–1992 as a residual of (a) and precipitation corresponding to the period.

where W represents the precipitable water (i.e., column integrated water vapor), and Q is the water vapor flux convergence in the atmosphere (Fig. 1.5a); all fluxes given in the unit volume of per time step). Since the atmospheric water content in both solid and liquid phases is generally small, only the water vapor is considered in equation (1.2). Figure 1.4b shows that the water storage in an atmospheric column is increased by the lateral convergence of water vapor and evapotranspiration from the bottom of the column (i.e., land surface), and decreases due to the precipitation falling from the bottom of the atmosphere column to the land.

Since there are common terms in equations (1.1) and (1.2), they can be combined into:

$$-\frac{dW}{dt}+Q=\left(P-E\right)=\frac{dS}{dt}+R \qquad (1.3)$$

Figure 1.4c illustrates the balance in this equation. The difference of precipitation and evapotranspiration is equal to the sum of the decrease of atmospheric water vapor storage and lateral (horizontal) convergence, and is also equal to the sum of the increase of water storage over the land and runoff. Theoretically, equation (1.3) can be applied for any control volume of the land area combined with the atmosphere above, however, the practical applicability depends on the accuracy and availability of atmospheric and hydrologic information. The global distribution of total evapotranspiration is shown in Figure 1.5b, which is estimated using the atmospheric water balance. *Trenberth et al.* [2007] used 40 yr ECMWF Re-Analysis [ERA-40; *Uppala et al.*, 2005] to compute the atmospheric moisture budget (i.e., *E–P*) and calculated global evapotranspiration as a residual of the precipitation and runoff (i.e., *P–E*) using gauged streamflow data of the largest 921 rivers in the world. This approach has been extended combining terrestrial water storage variability (obtained from remote sensing data by Gravity Recovery and Climate Experiment, GRACE; *Tapley et al.*, 2004) and satellite altimetry-based ocean mass change observation to estimate basin-scale evapotranspiration [*Rodell et al.*, 2004], global terrestrial discharges [*Syed et al.*, 2010], and discharges in continents and large river basins [*Syed et al.*, 2009].

1.4. MACROSCALE MODELING FOR WATER CYCLE IN NATURE

Macroscale hydrological models have been developed in response to societal expectations for solving current and future world water issues. There is an increasing demand for information on water resources and the prediction of their future changes. Conventionally, available freshwater resources are commonly defined as annual runoff estimated by historical river discharge data or water-balance calculation [*Baumgartner and Reichel*, 1975; *Korzun*, 1978]. Such an approach has been used to provide valuable information on annual freshwater resources in many countries. Atmospheric water balance using the water vapor flux convergence could alternatively be used to estimate global distribution of runoff based on the atmospheric reanalysis and data assimilation system [*Oki et al.*, 1995].

In the early 1990s, during the planning stage of the GEWEX Asian Monsoon Experiment (GAME), the topic "how to develop macroscale hydrological models" was discussed among Japanese scientists based on land-atmosphere interaction studies. Two approaches were identified. The first approach was to extend a conventional microscale rainfall-runoff hydrological model to a macroscale model that could run on the continental scale with a detailed energy balance and vegetation representation. The other approach was to enhance hydrological processes in land surface models (LSMs) and couple them with horizontal water flow processes, particularly with river flow.

The land surface model was originally devised as a physical scheme of a GCM to provide appropriate lower boundary conditions of land grid boxes [*Pitman*, 2003]. The first implementation, the so-called bucket model, has a globally constant soil depth and moisture-holding capacity, and determines the Earth's surface temperature using a simple heat balance equation [*Manabe* 1969]. Evaporation in the bucket model is simply determined by a linear relationship with soil moisture availability. *Deardorff* [1978] used the "force-restore" method for soil scheme and proposed a "big leaf" type for vegetation representation that has a single layer canopy for heat and moisture exchanges characterized by the micrometeorological bulk parameters. The big leaf canopy model has been broadly adopted in so-called second generation LSM including the Biosphere Atmosphere Transfer Scheme [BATS; *Dickinson et al.*, 1986] and Simple Biosphere Model [SiB; Sellers *et al.*, 1986]. After a major advance of the second generation LSMs, which explicitly considered a vegetation cover on the Earth's surface, LSMs were able to simulate the carbon cycle. Representation of plant physiology enabled LSMs such as SiB2 [*Sellers et al.*, 1996a] to control carbon and water fluxes simultaneously, taking into account light, carbon dioxide, and water stresses. Although third generation LSMs tended to employ multiple soil layers and simulated better underground processes of vertical heat and moisture transfer, intergrid exchanges such as "river", a horizontal redistribution of water, were not considered.

Oki and Sud [1998] developed a global river channel network named Total Runoff Integrating Pathway (TRIP). *Oki et al.* [1999] proposed a framework for evaluating global water cycles via off-line (uncoupled with atmosphere) simulation of LSMs combined with river routing schemes as a post-processors. The accuracy of global water balance estimated by 11 land surface models (LSMs) was validated by river discharge utilizing TRIP. The framework is also useful for translating climate change–driven changes in hydrological cycles (projected by GCMs) into socially relevant information, such as changes in future world-water resources and the frequency of flood and drought [e.g., *Nohara et al.*, 2006; *Hirabayashi et al.*, 2008; *Hirabayashi and Kanae*, 2009; *Hirabayashi et al.*, 2013]. The second phase of the Global Soil Wetness Project (GSWP2) also utilized such framework [*Dirmeyer et al.*, 2006]. A comprehensive review of the global hydrologic cycle was done and world-water resources were estimated. TRIP and the river routing scheme were widely adopted by several GCMs in the world, including the European Centre for Medium-Range Weather Forecasts (ECMWF) for flood forecasting applications [*Pappenberger et al.*, 2010]. Six out of 23 future projections in the fourth assessment report of the Intergovernmental Panel on Climate Change (IPCC) utilized TRIP to identify the impact of climate change on hydrological cycles [*Faloon and Betts*, 2006]. The global river-routing scheme, TRIP, was fundamentally revised recently. The new scheme, named CaMa-Flood, which adopts the diffusive equation as its principal equation, has the capability to represent natural inundation processes [*Yamazaki et al.*, 2011]. However, its couplings with large water bodies (e.g., lakes), human interventions (e.g., reservoir operations), and evaporation from water surfaces are still under development.

Kim et al. [2009] suggested another framework to evaluate off-line hydrological simulations not only using single flux term (i.e., discharge) but also including total terrestrial water storage (TWS) variations, which consist

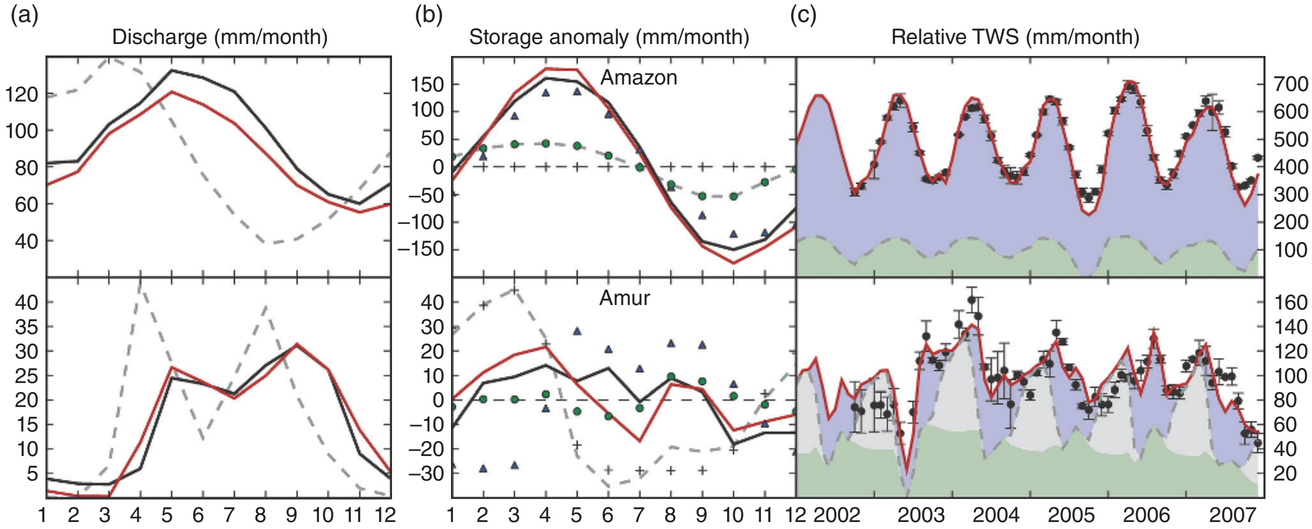

Figure 1.6 Basinwise validation for a macroscale hydrological simulation using the gauged Global Runoff Data Center (GRDC) discharge and the observed TWSA by GRACE. It shows (a) seasonal variations of GRDC discharge (black solid line), simulated discharge (red solid line), and runoff without routing (gray dashed line); (b) seasonal variations of GRACE observed TWSA (black solid line), simulated TWSA with river storage (red solid line), simulated TWSA without river storage (gray dashed line), and the major water storage components in TWS; and (c) interannual variations of relative TWS: the GRACE observation (black dot), simulation with river storage (red solid line), and simulation without river storage (gray dashed line). Gray crosses and shade, green circles and shade, and blue triangles and shade in (b) and (c) represent the individual storage component of snow water, soil moisture, and river storage, respectively [from *Kim et al.*, 2009].

of soil moisture, snow water, and river water (Fig. 1.6). As the satellite mission GRACE has monitored TWS with unprecedented accuracy since 2002, it became feasible to validate the partition of terms in terrestrial water balance [*Famiglietti and Rodell*, 2013]. Also, it was found that river storage not only explains different portions of total TWS variations but also plays different roles in different climatic regions. River is the most dominant water-storage component in wet basins (e.g., Amazon) in terms of amplitude and acts as a “buffer” which smooths the seasonal variation of total TWS especially in snow-dominated basins (e.g., Amur, Lena, Yenisei).

The model simulation of TWS may not be able to reproduce the amplitude and seasonal pattern of observed TWS variations by GRACE without an appropriate representation of a river storage component. Also, using a geodesy approach, *Han et al.* [2009] employed a set of TRIP simulations using different effective velocities in the Amazon River Basin and its vicinity. The model simulations were compared to the residual of GRACE L1b measurements derived from removing all the gravity-influencing factors except for the lateral redistribution of water storage in the Amazon river network. They demonstrated that the optimal flow velocity of TRIP in the Amazon varies between rising and falling water levels.

The global off-line hydrological modeling framework has been used to estimate large-scale water cycles since it is still the only available methodology that covers the global area for a sufficient time span without any gap. To reduce or estimate simulation uncertainties, approaches such as data model integration (e.g., data assimilation) and multimodel ensemble (MME) have been proposed. The Making Earth System Data Records for Use in Research Environments (MEaSUREs) project compiled various sources of data set including remote sensing, atmospheric reanalysis and model simulations, and optimized sets of flux terms using a data assimilation technique [*Rodell et al.*, 2015]. MME approach has been frequently performed as a community effort. International model intercomparison projects (MIPs) such as Global Soil Wetness Project [GSWP; *Dirmeyer et al.*, 2006; *Dirmeyer*, 2011] and Water Model Intercomparison Project [WaterMIP; *Haddeland et al.*, 2011] are good examples adopting MME approach to quantify the fluxes of water cycles globally, and they are introduced in Section 1.6 with more details. Table 1.1 compares recent studies that estimate global water balance using different approaches.

1.5. CLIMATE CHANGE AND HUMAN IMPACT

Global concentrations of carbon dioxide and methane have grown from the latter part of the eighteenth century. Since then it has been called the “Anthropocene”

Table 1.1 Global Water Balance in mm yr^{-1} by Different Studies

	Type	Period	P	ET	R	ET/P
Oki and Kanae [2006]*	Model-based	1986–1995	826.5	**487.7**	**338.8**	0.59
GSWP2 (*Dirmeyer et al.* [2006])	Model-based	1986–1995	836.4	**488.4**	**348.0**	0.58
Trenberth et al. [2007]**	Observations	Varies by datasets	762.0	492.2	269.7	0.65
WaterMIP (*Harding et al.* [2011])	Model-based	1985–1999	872.0	**499.0**	**375.0**	0.57
Kim and Oki [2014]	Model-based	1979–2013	**757.0**	469.0	288.0	0.62
MEaSUREs (*Rodell et al.* [2015])	Observations and Model-based	2000–2010 (mostly)	795.7	**481.8**	313.9	0.61

Note: Boldface numbers indicate ensemble estimations.
* Original values in km^3yr^{-1} are divided by $1.34 \times 10^8 km^2$ (global land area excluding Antarctica).
** Original values in km^3yr^{-1} are divided by $1.48 \times 10^8 km^2$ (global land area including Antarctica).

[*Crutzen* 2002] as human activities have driven global environmental changes. Human activities have altered water flows and storages significantly during the past centuries by irrigation, damming, and groundwater extraction. Therefore, the "real" global water cycles are not "natural" anymore, and thus geoscience communities have been urged to consider the human impact in their analyses and the associated modeling systems. Simple analytical water-balance models have been widely used to estimate global-scale available freshwater resources in the world since the beginning of this century [*Alcamo et al.*, 2000; *Vörösmarty et al.*, 2000]. Later, LSMs were used to simulate global water cycles [*Oki et al.*, 2001; *Dirmeyer et al.*, 2006] and to assess global water resources by estimating the water demand under future climate change scenarios [*Shen et al.*, 2008]. Some of those estimates were calibrated by multiplying an empirical factor in the river basins where observed discharge data are available. However, recent model simulations with advanced climate forcing data can estimate global runoff distribution with adequate accuracy without the need for calibration [*Hanasaki et al.*, 2008a].

H08 is the genesis of the global hydrological model including human intervention modules. It includes a reservoir operation scheme [*Hanasaki et al.*, 2006] to simulate the "real" hydrological cycles that are significantly influenced by anthropogenic activities to modify "natural" hydrological cycles on the global scale in the Anthropocene. The integrated water resources model is further coupled with a crop growth submodel, which can simulate the timing and quantity of irrigation requirements, and a submodel, which can estimate environmental flow requirements [*Hanasaki et al.*, 2008a]. A similar approach is found in *Haddeland et al.* [2006], which was tested over North America and Asian regions within the framework of Variable Infiltration Capacity (VIC) [*Liang et al.*, 1994].

Döll et al. [2009] analyzed anthropogenic river flow alteration using a global hydrology and water-use model WaterGAP [*Alcamo et al.*, 2003] in a global scale and found significant decrease and increase of the monthly statistical low river discharge (Q_{90}) on 26% and 5% of the land area. Such an approach can assess the balance of water demand and supply on a daily timescale.

A gap in the subannual distribution of water availability and water use can be detected in the Sahel, the Asian monsoon region and southern Africa, where conventional water scarcity indices such as the ratio of annual water withdrawal to water availability and available annual water resources per capita [*Falkenmark and Rockström*, 2004] cannot properly detect the stringent balance between demand and supply [*Hanasaki et al.*, 2008b]. However, the capability of future projections of the water demand side is relatively poor; nevertheless, *Hanasaki et al.* [2013] illustrated future water deficits considering both climatic and social changes.

Further development of water demand and usage models considering various social constraints based on field survey and data collection are needed to reduce uncertainty and improve the reliability of future projections. In addition, better representation of human interventions in land surface models is expected to improve the accuracy of the estimates of global hydrological cycles. Recently, the human intervention components of the H08 model were transplanted into an LSM Minimal Advanced Treatments of Surface Interaction and RunOff (MATSIRO) [*Takata et al.*, 2003], which was then applied to assess the impact of changes in terrestrial water storage due to unsustainable groundwater use, artificial reservoir water impoundment, and climate-driven natural variabilities in global mean sea level [*Pokhrel et al.*, 2012], even though their estimates are larger than other estimates [*Aeschbach-Hertig and Gleeson*, 2012].

Numerical models can be associated with a scheme backtracking the origin and flow path by tracing the isotopic ratio of water [*Yoshimura et al.*, 2004]. Such a flow-tracing function of water in the integrated water resources model [*Hanasaki et al.*, 2008a] considering the sources of water withdrawal from stream flow, medium-sized reservoirs, and nonrenewable groundwater in addition to

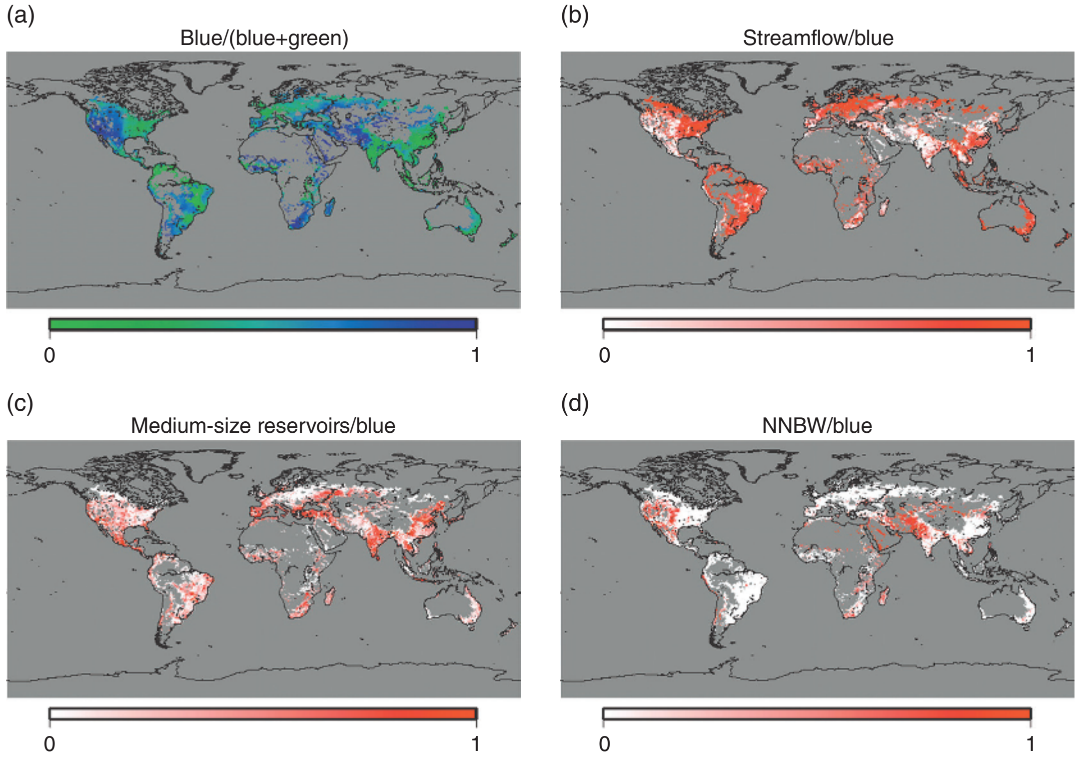

Figure 1.7 (a) The ratio of blue water to the total evapotranspiration during a cropping period from irrigated cropland (the total of green and blue water). The ratios of (b) streamflow, (c) medium-size reservoirs, and (d) nonrenewable and nonlocal blue-water withdrawals to blue water [from *Hanasaki et al.*, 2010].

precipitation to croplands enabled the assessment of the origin of water producing major crops [*Hanasaki et al.*, 2010]. Figure 1.7 shows that areas highly dependent on nonrenewable groundwater are detected in Pakistan, Bangladesh, the western part of India, the north and western parts of China, some regions in the Arabian Peninsula and the western part of the United States through Mexico. These regions are also detected as "hot spots" of groundwater depletion in an overview by *Wada et al*. [2010], which used a global hydrological model PCRaster-GLOBal Water Balance [*Van Beek and Bierkens*, 2009] to assess groundwater abstraction in excess of recharge.

Cumulative nonrenewable groundwater withdrawals estimated by the model correspond fairly well to the country statistics of total groundwater withdrawals. This integrated model has the ability to quantify the global virtual water flow [*Allan*, 1998; *Oki and Kanae*, 2004] or "water footprint" [*Hoekstra and Chapagain*, 2007] through major crop consumption [*Hanasaki et al*., 2010]. Additionally, a tracer scheme allows tracking of the shift of water pathways along with the shift of climate regime. Since the water pathways and their changes are essential information for regional water resource and disaster management, their future shifts should be effectively integrated to the adaptation and mitigation strategy to climate change [*IPCC*, 2012].

1.6. INTERNATIONAL COLLABORATION AND CAPACITY BUILDING

In the early 1990s, the Project for Intercomparison of Land-Surface Parameterization Schemes (PILPS) was carried out in order to evaluate and improve land surface schemes for climate and weather prediction models [*Henderson-Sellers et al*., 1995; *Henderson-Sellers et al*., 1996; *Pitman and Henderson-Sellers*, 1998]. As a research activity of the World Climate Research Programme (WCRP) sponsored by the Global Energy and Water Cycle Experiments Project (GEWEX) and the Working Group on Numerical Experimentation (WGNE), PILPS covers a broad range of intercomparison works from offline to coupled experiments. PILPS is a remarkable contribution to the research communities as it incorporates documentation, intercomparison, and validation of a large number of participating parameterization schemes for different process regimes such as surface, soil, and snow. However, the experiment design was not extended to produce a comprehensive data set using global-scale off-line simulations, which is an indispensable data source for increasing the depth of our understanding of global hydrological cycles and water resources.

GSWP is the first global MME analysis of fluxes and state variables in land surface processes [*Dirmeyer et al.*, 2006], as a project of Global Land/Atmosphere System Study (GLASS), which is a science panel of GEWEX/WCRP. The original research objective of GSWP was to provide a GCM with realistic variabilities of land boundary conditions, since they were not operationally monitored, unlike the oceans (e.g., sea surface temperature). Phase 1 and phase 2 of the project were linked to the International Satellite Land Surface Climatology Project (ISLSCP) Initiative I for 1987–1988 [*Sellers et al.*, 1996b] and Initiative II for 1986–1995 [*Hall et al.*, 2001], respectively. NCEP/NCAR (National Centers for Environmental Prediction/National Center for Atmospheric Research) atmospheric reanalysis data [*Kalnay et al.*, 1996] and globally available observational products [e.g., Global Precipitation Climatology Centre (GPCC); *Rudolf et al.*, 1994] were combined to generate meteorological boundary conditions to force land-surface models in a standalone off-line mode. GSWP demonstrated the capacity and the feasibility of an international collaborative research framework to evaluate state-of-the-art land surface models and to integrate them into a comprehensive dataset of global energy and water cycles.

Water and Global Change [WATCH; *Harding et al.*, 2011] was an international initiative to interface hydrology and climate sciences for further understanding on current and future water cycles at the global scale. As a key data set, WATCH Forcing Data [*Weedon et al.*, 2011] was developed based on ERA-40 atmospheric reanalysis by ECMWF. Monthly observations of global surface meteorological variables by Climate Research Unit [CRU; *New et al.*, 1999, 2000] were used mainly to correct the biases of the reanalysis product. As a core of the WATCH project, WaterMIP [*Haddeland et al.*, 2011] compared different classes of models including six land surface models and five global hydrological models at global 0.5° land grids for a 15 yr period (1985–1999). WaterMIP showed considerable range of ensemble spreads for simulated water flux variables (e.g., 45% of mean simulated runoff) due to different model realizations, which implies climate change impact studies need to incorporate not only multiple climate model but also multiple impact models.

The Inter-Sectoral Impact Model Intercomparison Project (ISI-MIP) was launched to synthesize the impact of future climate change quantitatively. Unlike previous studies on the impact assessment of climate change, it deals with impact through multiple sectors including water, ecosystem, agriculture and health at different levels of global warming [*Warszawski et al.*, 2014]. The fast track of the project successfully delivered a systematic overview of climate change and human impact across those sectors [*Piontek et al.*, 2014]. However, it also confirmed that the state-of-the-art impact models are still accompanied with huge uncertainty due to their model structures [*Schewe et al.*, 2014], which means that further effort is needed for model development, otherwise it will fail to draw a proper analysis for our society.

Recently, the third phase of GSWP (GSWP3) was proposed with extended science questions: (1) What will be the balance and variability of the hydro-energy-eco system over land in 20th and 21st centuries? (2) How the interactions between natural processes have changed in a long-term period under changing climate in the Anthropocene? (3) How do the state-of-the-art land-surface models perform and how can they be improved?

To answer those questions, GSWP3 has an experiment design that consists of long-term retrospective (EXP1; 1850 to present), long-term future climate (EXP2; present to 2100), and a short-term super ensemble (EXP3; 1979 to present). Through the project, a century-long comprehensive data set of energy, water, and carbon cycles will be produced with appropriate model verifications in ensemble land simulations in order to investigate the long-term changes of their components and interactions. It can also contribute to model evaluations. By including a wide range of land-surface, hydrologic, and ecological models, the impacts of missing/included processes and model uncertainty can be investigated.

For the long-term retrospective experiment, the century-long (1901–2010) meteorological forcing data set was generated using 20th Century Reanalysis (20CR) [*Compo et al.*, 2011] and globally available observational products such as GPCC and CRU for surface meteorological variables. To achieve further realistic variability and resolve known problems (e.g., Gibbs phenomena) within 20CR, global spectral nudging dynamical downscaling [*Yoshimura and Kanamitsu*, 2008; *Hong and Chang*, 2012] and daily scale-bias correction techniques were applied. The original reanalysis was dynamically downscaled into global T248 (~0.5°) resolution with adding values in the spatiotemporal domain of high frequency while keeping low frequency signal in the mean state and spatiotemporal variability, in comparison with previous bias correction methods. Currently, the long-term retrospective experiment is under way, and it is expected to deliver the first results in 2016.

The Land Surface, Snow, and Soil-moisture Model Intercomparison Project (LS3MIP) is a CMIP6-endorsed MIP under development. In the context of the CMIP6, LS3MIP will provide a comprehensive assessment of land-climate feedbacks and diagnoses of the land-surface schemes of current ESMs with uncertainty quantifications to better constrain climate change projections, particularly for highly vulnerable regions (e.g., densely populated regions, polar regions, agricultural areas, and land ecosystems) [*Seneviratne et al.*, 2014]. It will embrace a small number of multimodel experiments and simulations driven in off-line mode (land surface only). It will be coupled to the atmosphere (driven by prescribed sea surface temperatures) and embedded in fully coupled Atmosphere-Ocean GCMs. The experiments are divided into two parts, the first one addressing land systematic biases (LMIP, building upon GSWP3 experiment) and the second addressing land feedbacks in an integrated framework (LFMIP, building upon the ESM-snowMIP and GLACE-CMIP blueprints).

LS3MIP will contribute to reducing the systematic biases from the land-surface component of climate models and a better representation of feedback mechanisms related to snow and soil moisture in climate models. It will lead to the improvement of climate change projections and further contribute to the assessment of the possible changes and impacts of climate changes in the next cycle (Sixth Assessment Report) of the Intergovernmental Panel on Climate Change.

1.7. PROSPECTS FOR GLOBAL HYDROLOGY AND MODEL DEVELOPMENT

The field of global hydrology today has certainly evolved from the time it was established after "The Forgotten Earth Science" by *Bras et al.* [1987], which led to the call for greater prominence. Current hydrology has the capability to monitor, understand, and predict global hydrological cycles of social-ecological systems, combining both human and natural systems. However, there are still challenging scientific issues to be resolved in global hydrology and model development. Here, some examples are briefly described. A review of global hydrology from different perspectives can be found also in *Bierkens* [2015].

Hyper-resolution modeling (~1 km globally) is one potential path forward [e.g., *Wood et al.*, 2011]. Because of the very rapid development of computer and information technology, currently available computational resource is capable of simulating global nonhydrostatic atmospheric simulation with up to 870 m mesh [*Miyamoto et al.*, 2013]. However, refinements of detailed natural and anthropogenic processes should be promoted with the consideration of the scale dependency of the governing equations and numerical implementation. Maintenance and development of global monitoring networks and data sharing protocol are necessary for better simulations and verification. Also, data handling interface and geolocated visualization for big data will be beneficial to our society.

Implementation of missing components is one of the basic strategies in model development. Numerical implementations of individual processes are diverse among modeling groups because their aims and priorities are not necessarily identical. However, a common problem exists in macroscale simulation frameworks, that is, the model needs to include more detailed processes in order to be more accurate, for example, (1) decomposition of evapotranspiration (i.e., transpiration, interception loss, and bare soil evaporation); (2) three-dimensional dynamics of groundwater and hill-slope processes and associated runoff separation (i.e., surface runoff, base flow); (3) processes in semiarid regions and tropics; (4) snow and glaciers in complex terrains (e.g., timing of snow melt, permafrost, ice sheet movement/melting, and aging/albedo change); (5) separation of rain and snow; (6) salty water–freshwater exchanges (i.e., submarine freshwater discharge and salinization); and (7) light and water use efficiency of vegetation and the impacts of CO_2 fertilization.

Although increasing the integration level within a modeling framework is indispensable to understand forces and feedbacks in nonlinear systems, in general, the state-of-the-art models do not have a fully coupled modular structure. For examples, river routing schemes in many land-surface models do not exchange heat and water with the atmosphere (i.e., through precipitation and evaporation) and ground (i.e., through infiltration and recharge). Also, the information is conveyed "one way" during simulations for climate change impact assessment, since most impact models are post-processors, referring to natural cycles simulated by climate model and hydrological model. However, it is important to consider interactive processes between human and nature for realistic estimations in the Anthropocene.

REFERENCES

Aeschbach-Hertig, W., and T. Gleeson (2012), Regional strategies for the accelerating global problem of groundwater depletion, *Nature Geosci.*, *5*, 853–860.

Alcamo, J., P. Döll, T. Henrichs, F. Kaspar, B. Lehner, T. Rösch, and S. Siebert (2003), Development and testing of the WaterGAP2 global model of water use and availability, *Hydrol. Sci. J.*, *48*, 317–337.

Alcamo, J., T. Henrichs, and T. Rösch (2000), *World Water in 2025–Global modelling and scenario analysis for the World Commission on Water for the 21st Century, Tech.* Report, Centre for Environmental Systems Research, University of Kassel, Kassel, Germany.

Allan, J. A. (1998), Virtual Water: A strategic resource, global solution to regional deficits, *Groundwater*, *36*(4), 545–546.

Baumgartner, F., and E. Reichel (1975), *The World Water Balance: Mean Annual Global, Continental and Maritime Precipitation, Evaporation and Runoff*, pp. 179, Munchen, Ordenbourg.

Bierkens, M. F. P. (2015), Global hydrology 2015: State, trends, and directions, *Water Resour. Res.*, *51*, 4923–4947.

Bras, R., P. S. Eagleson, E. K. Turner, and R. M. Parsons (1987), Hydrology, The forgotten Earth science, EOS Trans, *Amer. Geophys. Union*, *68*, 227.

Compo, G. P., and Coauthors (2011), The twentieth century reanalysis project. *Quart. J. Roy. Meteor. Soc.*, *137*(654), 1–28.

Crutzen, P. J. (2002), Geology of mankind—the Anthropocene, *Nature*, *415*, 23.

Deardorff, J. W. (1978), Efficient prediction of ground surface temperature and moisture with inclusion of a layer of vegetation, *J. Geophys. Res.*, *83*, 1889–1903.

Dickinson, R. E., A. Henderson-Sellers, P. J. Kennedy, and M. F. Wilson (1986), Biosphere–Atmosphere Transfer Scheme (BATS) for the NCAR Community Climate Model. NCAR Technical Note TN-275 + STR.

Dirmeyer, P. A. (2011), A History and Review of the Global Soil Wetness Project (GSWP), *J. Hydrometeor.*, *12*, 729–749.

Dirmeyer, P. A., X. A. Gao, M. Zhao, Z. C. Guo, T. Oki, and N. Hanasaki (2006), GSWP-2 multimodel anlysis and implications for our perception of the land surface, *Bull. Amer. Meteor. Soc.*, *87*, 1381–1397.

Döll, P., K. Fiedle r, and J. Zhang (2009), Global-scale analysis of riverflow alterations due to water withdrawals and reservoirs, *Hydrol. Earth Syst. Sci.*, *13*, 2413–2432, doi:10.5194/hess-13-2413-2009.

Falkenmark, M., and J. Rockström (2004), *Balancing Water for Humans and Nature*, Earthscan, London, UK.

Falloon, P. D., and R. A. Betts (2006), The impact of climate change on global river flow in HadGEM1 simulations, *Atmos. Sci. Let.*, *7*, 62–68.

Famiglietti, J. S., and M. Rodell (2013), Water in the balance, *Science*, *340*, 1300–1301.

Haddeland, I., D. B. Clark, W. Franssen, F. Ludwig, F. Voß, N. W. Arnell, N. Bertrand, M. Best, S. Folwell, D. Gerten, S. Gomes, S. N. Gosling, S. Hagemann, N. Hanasaki, R. Harding, J. Heinke, P. Kabat, S. Koirala, T. Oki, J. Polcher, T. Stacke, P. Viterbo, G. P. Weedon, and P. Yeh (2011), Multimodel estimate of the global terrestrial water balance: setup and first results, *J. Hydrometeor.*, *12*, 869–884.

Haddeland, I., T. Skaugen, and D. P. Lettenmaier (2006), Anthropogenic impactson continental surface water fluxes, *Geophys. Res. Lett.*, *33*,L08406, doi:10.1029/2006GL026047.

Hall, F. G., B. Meeson, S. Los, and E. Brown de Colstoun (2001), ISLSCP II: New 10+ year multi-parameter near-surface global data set—Including greater carbon and vegetation data. *GEWEX News*, Vol. *11*, No. 2, International Gewex Project Office, Silver Spring, MD, 12–13.

Han, S.-C., H. Kim, I.-Y. Yeo, P.-J. Yeh, T. Oki, K.-W. Seo, D. Alsdorf, and S. B. Luthcke (2009), Dynamics of surface water storage in the Amazon inferred from measurements of inter-satellite distance change, *Geophys. Res. Lett.*, *36*, L09403, doi:10.1029/2009GL037910.

Hanasaki, N., S. Kanae, and T. Oki (2006), A reservoir operation scheme for global river routing models, *J. Hydrol.*, *327*, 22–41.

Hanasaki, N., S. Kanae, T. Oki, K. Masuda, K. Motoya, N. Shirakawa, Y. Shen, and K. Tanaka (2008a), An integrated model for the assessment of global water resources–part 1: Model description and input meteorological forcing, *Hydrol. Earth Syst. Sci.*, *12*, 1007–1025.

Hanasaki, N., S. Kanae, T. Oki, K. Masuda, K. Motoya, N. Shirakawa, Y. Shen, and K. Tanaka (2008b), An integrated model for the assessment of global water resources–part 2: Applications and assessments, *Hydrol. Earth Syst. Sci.*, *12*, 1027–1037.

Hanasaki, N., T. Inuzuka, S. Kanae, and T. Oki (2010), An estimation of global virtual water flow and sources of water withdrawal for major crops and livestock products using a global hydrological model, *J. Hydrol.*, *384*, 232–244, doi:10.1016/j.jhydrol.2009.09.028.

Hanasaki, N., S. Fujimori, T. Yamamoto, S. Yoshikawa, Y. Masaki, Y. Hijioka, M. Kainuma, Y. Kanamori, T. Masui, K. Takahashi, and S. Kanae (2013), A global water scarcity assessment under Shared Socio-economic Pathways – Part 2: Water availability and scarcity, *Hydrol. Earth Syst. Sci.*, *17*, 2393–2413.

Harding, R., M. Best, E. Blyth, S. Hagemann, P. Kabat, L. M. Tallaksen, T. Warnaars, D. Wiberg, G. P. Weedon, H. van Lanen, F. Ludwig, and I. Haddeland (2011), WATCH: Current Knowledge of the Terrestrial Global Water Cycle, *J. Hydrometeor.*, *12*, 1149–1156.

Henderson-Sellers, A., A. J. Pitman, P. K. Love, P. Irannejad, and T. Chen (1995), The project for Intercomparison of land surface parameterisaton schemes PILPS) Phases 2 and 3, *Bull. Amer. Meteor. Soc.*, *76*, 489–503.

Henderson-Sellers, A., K. McGuffie, and A. J. Pitman (1996), The project for intercomparison of land-surface parametrization schemes (PILPS): 1992 to 1995, *Climate Dynamics*, *12*(12), 849–859.

Hirabayashi, Y., and S. Kanae (2009), First estimate of the future global population at risk of flooding, *Hydrolog. Res. Lett.*, *3*, 6–9.

Hirabayashi, Y., S. Kanae, S. Emori, T. Oki, and M. Kimoto (2008), Global projections of changing risks of floods and droughts in a changing climate, *Hydrolog. Sci. J.*, *53*(4), 754–772.

Hirabayashi, Y., R. Mahendran, S. Koirala, L. Konoshima, D. Yamazaki, S. Watanabe, and S. Kanae (2013), Global flood risk under climate change. *Nature Climate Change*, *3*, 816–821.

Hoekstra, A. Y., and A. K. Chapagain (2007), Water footprints of nations: Water use by people as a function of their consumption pattern, *Water Resour. Man.*, *21*, 35–48.

Hong, S. Y., and E. C. Chang (2012), Spectral nudging sensitivity experiments in a regional climate model, *Asia-Pacific J. Atmos. Sci.*, *48*(4), 345–355.

Hoskins, B. J. (1989), *Diagnostics of the global atmospheric circulation based on ECMWF analysis 1979–1989*, Tech. Rep. WCRP-27, WMO/TD-No.326, World Meteorological Organization.

Huffman, G. J., R. F. Adler, P. Arkin, A. Chang, R. Ferraro, A. Gruber, J. Janowiak, A. McNab, B. Rudolf, and U. Schneider (1997), The Global Precipitation Climatology Project (GPCP) Combined Precipitation Dataset, *Bull. Amer. Meteor. Soc.*, *78*, 5–20.

IPCC (2012), *Managing the Risks of Extreme Events and Disasters to Advance Climate Change Adaptation. A Special Report of Working Groups I and II of the Intergovernmental*

Panel on Climate Change [Field, C. B., V. Barros, T. F. Stocker, D. Qin, D. J. Dokken, K. L. Ebi, M. D. Mastrandrea, K. J. Mach, G.-K. Plattner, S. K. Allen, M. Tignor, and P. M. Midgley (eds.)]. Cambridge University Press, Cambridge, UK, and New York, NY, USA.

Kalnay, E., M. Kanamitsu, R. Kistler, W. Collins, D. Deaven, L. Gandin, M. Iredell, S. Saha, G. White, J. Woollen, Y. Zhu, A. Leetmaa, R. Reynolds, M. Chelliah, W. Ebisuzaki, W. Higgins, J. Janowiak, K. C. Mo, C. Ropelewski, J. Wang, R. Jenne, and D. Joseph (1996), The NCEP/NCAR 40-Year Reanalysis Project, *Bull. Amer. Meteor. Soc.*, *77*, 437–471.

Kim, H., and T. Oki (2014), [Global climate] River discharge [in "State of the Climate in 2013"]. *Bull. Amer. Meteor. Soc.*, *95* (7), S23–S24.

Kim, H., P. J.-F. Yeh, T. Oki, and S. Kanae (2009), Role of rivers in the seasonal variations of terrestrial water storage over global basins, *Geophys. Res. Lett.*, *36*, L17402, doi:10.1029/2009GL039006.

Koirala, S. (2010), *Explicit representation of groundwater process in a global-scale land surface model to improve hydrological predictions*, Ph. D thesis, The University of Tokyo.

Korzun, V. I. (1978), *World Water Balance and Water Resources of the Earth – Studies and Reports in Hydrology, 25*, UNESCO, Paris.

Liang, X., D. P. Lettennmaier, E. F. Wood, and S. J. Burges (1994), Asimple hydrologically based mo del o f land surface water and energyfluxes for general circulation models, *J. Geophys. Res.*, *99*(D7),14,415 – 14,428.

Manabe, S. (1969), Climate and the Ocean Circulation 1: I, The atmospheric circulation and the hydrology of the Earth's surface, *Monthly Weather Rev.*, *97*(11), 739–774.

Miyamoto, Y., Y. Kajikawa, R. Yoshida, T. Yamaura, H. Yashiro, and H. Tomita (2013), Deep moist atmospheric convection in a subkilometer global simulation, *Geophys. Res. Lett.*, *40*(18), 4922–4926.

New, M. G., M. Hulme, and P. D. Jones (1999), Representing twentieth-century space–time climate variability. Part I: Development of a 1961–90 mean monthly terrestrial climatology. *J. Climate*, *12*, 829–856.

New, M. G., M. Hulme, and P. D. Jones (2000), Representing twentieth-century space–time climate variability. Part II: Development of 1901–96 Monthly grids of terrestrial surface climate. *J. Climate*, *13*, 2217–2238.

Nohara, D., A. Kitoh, M. Hosaka, and T. Oki (2006), Impact of climate change on river discharge projected by multi-model ensemble, *J. Hydrometeor.*, *7*, 1076–1089.

Oki, T., and S. Kanae (2004), Virtual water trade and world water resources, *Water Sci. Tech.*, *49*(7), 203–209.

Oki, T., and S. Kanae (2006), Global hydrological cycles and world water resources, *Science*, *313*(5790), 1068–1072.

Oki, T., and Y. C. Sud (1998), Design of Total Runoff Integrating Pathways (TRIP) A global river channel network, *Earth Interact.*, *2*, 1–37.

Oki, T., D. Entekhabi, and T. I. Harrold (2004), The global water cycle, 225–257, in *State of the Planet: Frontiers and Challenges in Geophysics*, edited by R. S. J. Sparks and C. J. Hawkesworth, Geophysical Monograph Series, vol. 150, American Geophysical Union, Washington, D.C.

Oki, T., K. Musiake, H. Matsuyama, and K. Masuda (1995), Global atmospheric water balance and runoff from large river basins, *Hydrolog. Processes*, *9*, 655–678.

Oki, T., T. Nishimura, and P. Dirmeyer (1999), Assessment of annual runoff from land surface models using Total Runoff Integrating Pathways (TRIP), *J. Meteor. Soc. Japan*, *77*, 235–255.

Oki, T., Y. Agata, S. Kanae, T. Saruhashi, D. W. Yang, and K. Musiake (2001), Global assessment of current water resources using total runoff integrating pathways, *Hydrol. Sci. J.*, *46*, 983–995.

Pappenberger, F., H. L. Cloke, G. Balsamo, T. Ngo-Duc, and T. Oki (2010), Global runoff routing with the hydrological component of the ECMWF NWP system, *Int. J. Climatol.*, *30*(14), 2155–2174.

Piontek, F., C. Muller, T. Pugh, D. B. Clark, D. Deryng, J. Elliott, F. D. C. Gonzalez, M. Florke, C. Folberth, W. Franssen, K. Frieler, A. D. Friend, S. N. Gosling, D. Hemming, N. Khabarov, H. Kim, M. R. Lomas, Y. Masaki, M. Mengel, A. Morse, K. Neumann, K. Nishina, S. Ostberg, R. Pavlick, A. C. Ruane, J. Schewe, E. Schmid, T. Stacke, Q. Tang, Z. D. Tessler, A. M. Tompkins, L. Warszawski, D. Wisser, H. J. Schellnhuber (2014), Multisectoral climate impact hotspots in a warming world, *Proc. Nat. Acad. Sci.*, *111*(9), 3233–3238.

Pitman, A. J. (2003), The evolution of, and revolution in, land surface schemes designed for climate models, *Int. J. Climatol.*, *23*, 479–510.

Pitman, A. J., and A. Henderson-Sellers (1998), Recent progress and results from the project for the intercomparison of land surface parameterization schemes, *J. Hydrol.*, *212*, 128–135.

Pokhrel, Y., N. Hanasaki, P. Yeh, T. Yamada, S. Kanae, and T. Oki (2012), Model estimates of sea-level change due to anthropogenic impacts on terrestrial water storage, *Nature Geosci.*, *5*, 389–392.

Rodell, M., H. K. Beaudoing, T. S. L'Ecuyer, W. S. Olson, J. S. Famiglietti, P. R. Houser, R. Adler, M. G. Bosilovich, C. A. Clayson, D. Chambers, E. Clark, E. J. Fetzer, X. Gao, G. Gu, K. Hilburn, G. J. Huffman, D. P. Lettenmaier, W. T. Liu, F. R. Robertson, C. A. Schlosser, J. Sheffield, and E. F. Wood (2015), The observed state of the water cycle in the early twenty-first century, *J. Climate*, *28*, 8289–8318.

Rodell, M., J. S. Famiglietti, J. Chen, S. I. Seneviratne, P. Viterbo, S. Holl, and C. R. Wilson (2004), Basin scale estimate of evapotranspiration using GRACE and other observations, *Geophys. Res. Lett.*, *31*, L20504, doi:10.1029/2004GL020873.

Rudolf, B., H. Hauschild, W. Reuth, and U. Schneider (1994), Terrestrial precipitation analysis: Operational method and required density of point measurements, in *Global Precipitation and Climate Change*, edited by M. Desbois and F. Desalmond, NATO ASI Series I, Vol *26*, Springer-Verlag, 173–186.

Schewe, J., J. Heinke, D. Gerten, I. Haddeland, N. W. Arnell, D. B. Clark, R. Dankers, S. Eisner, B. M. Fekete, F. J. Colón-González, S. N. Gosling, H. Kim, X. C. Liu, Y. Masaki, F. T. Portmann, Y. Satoh, T. Stacke, Q. Tang, Y. Wada, D. Wisser, T. Albrecht, K. Frieler, F. Piontek, L. Warszawski, and P. Kabat (2014), Multimodel assessment of water scarcity under climate change, *Proc. Nat. Acad. Sci.*, *111*(9), 3245–3250.

Schneider, U., A. Becker, P. Finger, A. Meyer-Christoffer, M. Ziese, and B. Rudolf (2014), GPCC's new land surface precipitation climatology based on quality-controlled in situ data and its role in quantifying the global water cycle, *Theoret. App. Climatol.*, *115*, 15–40, doi: http://dx.doi.org/10.1007/s00704-013-0860-x.

Sellers, P. J., B. W. Meeson, J. Closs, J. Collatz, F. Corprew, D. Dazlich, F. G. Hall, Y. Kerr, R. Koster, S. Los, K. Mitchell, J. McManus, D. Myers, K.-J. Sun, and P. Try (1996a), The ISLSCP Initiative I Global Datasets: Surface Boundary Conditions and Atmospheric Forcings for Land-Atmosphere Studies, *Bull. Amer. Meteor. Soc.*, *77*, 1987–2005.

Sellers, P. J., D. A. Randall, C. J. Collatz, J. A. Berry, C. B. Field, D. A. Dazlich, C. Zhang, G. Collelo, and L. Bounoua (1996b), A revised land-surface parameterization (SiB2) for atmospheric GCMs. Part 1: model formulation, *J. Climate*, *9*, 676–705.

Sellers, P. J., Y. Mintz, Y. C. Sud, and A. Dalcher (1986), A Simple Biosphere model (SiB) for use within general circulation models, *J. Atmos. Sci.*, *43*, 505–531.

Seneviratne, S. I., B. van den Hurk, D. Lawrence, G. Krinner, G. Hurtt, H. Kim, C. Derksen, T. Oki, A. Boone, M. Ek, V. Brovkin, P. Dirmeyer, H. Douville, P. Friedlingstein, S. Hagemann, R. Koster, N. de Noblet-Ducoudre and A. Pitman (2014), Land processes, forcings, and feedbacks in climate change simulations: The CMIP6 LandMIPs. *GEWEX News*, *24*(4), Nov., 2014.

Shen, Y., T. Oki, N. Utsumi, S. Kanae, and N. Hanasaki (2008), Projection of future world water resources under SRES scenarios: water withdrawal, *Hydrol. Sci. J.*, *53*(1), 11–33.

Starr, V. P., and J. Peixöto (1958), On the global balance of water vapor and the hydrology of deserts, *Tellus*, *10*, 189–194.

Stubenrauch, C. J., W. B. Rossow, S. Kinne, S. Ackerman, G. Cesana, H. Chepfer, L. Di Girolamo, B. Getzewich, A. Guignard, A. Heldinger, B. C. Maddux, W. P. Menzel, P. Minnis, C. Pearl, S. Platnick, C. Poulsen, J. Riedi, S. Sun-Mak, A. Walther, D. Winker, S. Zen, and G. Zhao (2013), Assessment of global cloud data sets from satellites: Project and database initiated by the GEWEX radiation panel, *Bull. Amer. Metero. Soc.*, *94*(7), 1031–1049.

Syed, T. H., J. S. Famiglietti, and D. P. Chambers (2009), GRACE-based estimates of terrestrial freshwater discharge from basin to continental scales, *J. Hydrometeor.*, *10*, 22–40.

Syed, T. H., J. S. Famiglietti, D. P. Chambers, J. K. Willis, and K. Hilburn (2010), Satellite-based global-ocean mass balance estimates of interannual variability and emerging trends in continental freshwater discharge, *Proc. Nat. Acad. Sci.*, *107*, 17916–17921.

Takata, K., S. Emori, and T. Watanabe (2003), Development of minimal advanced treatments of surface interaction and runoff, *Global Planet. Change*, *38*, 209–222, doi:10.1016/S0921-8181(03)00030-4.

Tapley, B. D., S. Bettadpur, J. C. Ries, P. F. Thompson, and M. M. Watkins (2004), GRACE measurements of mass variability in the Earth system, *Science*, *305*(5683), 503–505, doi:10.1126/science.1099192.

Trenberth, K. E., L. Smith, T. Qian, A. Dai, and J. Fasullo (2007), Estimates of the global water budget and its annual cycle using observational and model data, *J. Hydrometeor.*, *8*, 758–769.

Uppala, S. M., P. W. Kållberg, A. J. Simmons, U. Andrae, V. Da Costa Bechtold, M. Fiorino, J. K. Gibson, J. Haseler, A. Hernandez, G. A. Kelly, X. Li, K. Onogi, S. Saarinen, N. Sokka, R. P. Allan, E. Andersson, K. Arpe, M. A. Balmaseda, A. C. M. Beljaars, L. Van De Berg, J. Bidlot, N. Bormann, S. Caires, F. Chevallier, A. Dethof, M. Dragosavac, M. Fisher, M. Fuentes, S. Hagemann, E. Hólm, B. J. Hoskins, L. Isaksen, P. A. E. M. Janssen, R. Jenne, A. P. McNally, J.-F. Mahfouf, J.-J. Morcrette, N. A. Rayner, R. W. Saunders, P. Simon, A. Sterl, K. E. Trenberth, A. Untch, D. Vasiljevic, P. Viterbo, and J. Woollen (2005), The ERA-40 re-analysis, *Quart. J. Roy. Meteor. Soc.*, *131*, 2961–3012.

van Beek, L. P. H., and M. F. P. Bierkens (2009), *The global hydrologicalmodel PCR-GLOBWB: Conceptualization, parameterization and verifi-cation, report*, Dep. of Phys. Geogr., Utrecht Univ., Utrecht, Netherlands.

Vörösmarty, C. J., P. Green, J. Salisbury, and R. B. Lammers (2000), Global water resources: vulnerability from climate change and population growth, *Science*, *289*(5477), 284–288.

Yamazaki, D., S. Kanae, H. Kim, and T. Oki (2011), A physically-based description of floodplain inundation dynamics in a global river routing model, *Water Resour. Res.*, *54*, doi: 10.1029/2010WR009726.

Yoshimura, K., and M. Kanamitsu (2008), Dynamical Global Downscaling of Global Reanalysis, *Monthly Weather Rev.*, *136*, 2983–2998, doi:10.1175/2008MWR2281.1.

Yoshimura, K., T. Oki, N. Ohte, and S. Kanae (2004), Colored moisture analysis estimates of variations in 1998 Asian monsoon water sources, *J. Meteor. Soc. Japan*, *82*, 1315–1329.

Wada, Y., L. P. H. van Beek, C. M. van Kempen, J. W. T. M. Reckman, S. Vasak, and M. F. P. Bierkens (2010), Global depletion of groundwater resources, *Geophys. Res. Lett.*, *37*, L20402, doi:10.1029/2010GL044571.

Warszawski, L., K. Frieler, V. Huber, F. Piontek, O. Serdeczny, and J. Schewe (2014), The Inter-Sectoral Impact Model Intercomparison Project (ISI–MIP): Project framework, *Proc. Nat. Acad. Sci.*, *111*(9), 3228–3232.

Weedon, G. P., S. Gomes, P. Viterbo, W. J. Shuttleworth, E. Blyth, H. Österle, J. C. Adam, N. Bellouin, O. Boucher, and M. Best (2011), Creation of the WATCH Forcing Data and Its Use to Assess Global and Regional Reference Crop Evaporation over Land during the Twentieth Century, *J. Hydrometeor*, *12*, 823–848.

Wood, E. F., J. K. Roundy, T. J. Troy, L. P. van Beek, M. F. Bierkens, E. Blyth, A. de Roo, P. Döll, M. Ek, J. Famiglietti, D. J. Gochis, N. van de Giesen, P. Houser, P. R. Jaffé, S. Kollet, B. Lehner, D. P. Lettenmaier, C. Peters-Lidard, M. Sivapalan, J. Sheffield, A. Wade, and P. Whitehead (2011), Hyperresolution global land surface modeling: Meeting a grand challenge for monitoring Earth's terrestrial water, *Water Resour. Res.*, *47*, W05301.